Electrochemical and structural studies of nickel(II) complexes with N_2O_2 Schiff base ligands
2. Crystal and molecular structure of *N,N'*-1,2-ethane-1,2-diyl-bis(2-hydroxyacetophenonylideneiminate)nickel(II), *N,N'*-1,2-*cis*-cyclohexane-1,2-diyl-bis(2-hydroxyacetophenonylideneiminate)-nickel(II) and *N,N'*-1,2-benzene-1,2-diyl-bis(3,5-dichlorosalicylideneiminate)nickel(II)

Fernando Azevedo[a], Maria A.A.F. de C.T. Carrondo[b,c,*], Baltazar de Castro[a,*], Maire Convery[b], Deolinda Domingues[a], Cristina Freire[a], M. Teresa Duarte[d,c], Kirsten Nielsen[b,c] and Isabel C. Santos[e]

[a]*Departamento de Química, Faculdade de Ciências, 4000 Porto (Portugal)*
[b]*Instituto de Tecnologia Química e Biológica, 2780 Oeiras (Portugal)*
[c]*Instituto Superior Técnico, 1000 Lisbon (Portugal)*
[d]*Centro de Química Estrutural, 1000 Lisbon (Portugal)*
[e]*Departamento de Química, ICEN-INETI, 2686 Sacavém (Portugal)*

(Received September 9, 1993; revised December 2, 1993)

Abstract

Reductive and oxidative chemistry of three complexes of formula [Ni(L)], where L represents a N_2O_2 Schiff base pseudomacrocyclic ligand based on salicylaldehyde derivatives and three different diamines, was studied in $(CH_3)_2SO$: *N,N'*-1,2-ethane-1,2-diyl-bis(2-hydroxyacetophenonylideneiminate)nickel(II) (**1**); *N,N'*-1,2-*cis*-cyclohexane-1,2-diyl-bis(2-hydroxyacetophenonylideneiminate)nickel(II) (**2**); *N,N'*-1,2-benzene-1,2-diyl-(bis(3,5-dichlorosalicylideneiminate)nickel(II) (**3**). Electrochemical behavior of the complexes was determined by cyclic voltammetry, and EPR spectroscopy was used to characterize the one-electron reduced/oxidized species. Reduction of the complexes **1** and **2** yielded Ni(I) complexes with a d_{xy} ground state ($g_z > g_x, g_y$), but the reduction of **3** is ligand-centered as suggested from the pseudo-isotropic radicalar EPR signal of frozen electrolyzed solutions. Oxidation of all three complexes is metal-centered and the oxidized products are low spin hexacoordinate Ni(III) species with two solvent molecules coordinated axially, with a d_{z^2} ground state ($g_x, g_y > g_z$). The crystal structures of the three Ni(II) complexes were determined from single crystal X-ray diffraction data collected with the use of Mo Kα radiation. **1**: space group *C2/c* with $a = 25.963(3)$, $b = 7.2973(4)$, $c = 17.357(2)$ Å, $\beta = 107.085(5)°$, $Z = 8$ ($R = 0.061$); **2**: space group $P2_1/a$ with $a = 9.645(6)$, $b = 19.149(16)$, $c = 10.743(5)$ Å, $\beta = 94.66(2)°$, $Z = 4$ ($R = 0.085$); **3**: space group $P2_1/n$ with $a = 13.372(5)$, $b = 8.785(2)$, $c = 16.534(5)$ Å, $\beta = 101.60(3)°$, $Z = 4$ ($R = 0.054$). Crystal packing of **1** and **3** involves the pairing of two centrosymmetrical related molecules in dimers, but that of **2** shows no systematic parallel orientation of any part of the molecules. X-ray structural data have provided a rationale for the $E_{1/2}$ values obtained for the reduction and oxidation processes.

Key words: Electrochemistry; Crystal structures; Nickel complexes; Schiff base ligand complexes

Introduction

Recent growing interest in the reductive and oxidative chemistry of nickel(II) macrocyclic complexes derives from recognition of the biological importance of the less common oxidation states of nickel and it involves the elucidation of factors that stabilize metal-centered reduced/oxidized species over ligand-based reduction/oxidation [1]. Work in our laboratory has attempted to assess how structural modifications on ligands will affect the reduction/oxidation site in nickel(II) complexes and develop a rationale to modulate redox

*Authors to whom correspondence should be addressed.

SSDI 0020-1693(94)03821-5

potentials of nickel(II) complexes with pseudomacrocyclic N_2O_2 Schiff base ligands [2, 3], and to compare the results obtained for these latter complexes with those that have already been identified to affect the redox behavior of nickel(II) tetraaza and porphyrinic macrocyclic complexes: chelate ring size/hole size [4, 5]; ring ruffling/axial ligation [6, 7]; degree and distribution of unsaturation [4, 8]; and substitution pattern in the chelate ring [4, 9].

In this paper we present the results of the structural determination of molecular and crystal structures of three nickel(II) complexes of general formula [Ni(L)], where L represents an N_2O_2 Schiff base pseudomacrocyclic ligand based on salicylaldehyde derivatives and three different diamines: *N,N'*-1,2-ethane-1,2-diyl-bis(2-hydroxyacetophenonylideneiminate)nickel(II) (**1**); *N,N'*-1,2-*cis*-cyclohexane-1,2-diyl-bis(2-hydroxyacetophenonylideneiminate)nickel(II) (**2**); *N,N'*-1,2-benzene-1,2-diyl-bis(3,5-dichlorosalicylideneiminate)-nickel(II) (**3**). Their electrochemical behavior on oxidation and on reduction was studied by cyclic voltammetry in $(CH_3)_2SO$. Spectroscopic characterizations of the one-electron oxidized/reduced species were performed by EPR to assess the site of electron transfer and a rationale for the redox behavior of these complexes was provided by the electronic and structural characteristics of the equatorial ligand.

Experimental

Reagents, solvents, ligands and complexes

All solvents used in the preparations were reagent grade (Merck). All reagents (nickel acetate tetrahydrate, *o*-phenylenediamine and ethylenediamine from Merck; 1,2-diaminecyclohexane, 2-hydroxyacetophenone and 3,5-dichlorosalicylaldehyde from Aldrich) were used as received, except ethylenediamine that was distilled prior to use.

The ligands *N,N'*-1,2-ethane-1,2-diyl-bis(2-hydroxyacetophenonylideneimine) [H_2-α,α'-Me_2salen] and *N,N'*-1,2-benzene-1,2-diyl-bis(3,5-dichlorosalicylideneimine) [H_2-3,5-Cl_2saloph], and the corresponding nickel(II) complexes ([Ni(α,α'-Me_2salen)] and [Ni(3,5-Cl_2saloph)]) were prepared and fully characterized as described elsewhere [2, 3]. The ligand *N,N'*-1,2-cyclohexane-1,2-diyl-bis(2-hydroxyacetophenonylideneimine) [H_2-α,α'-Me_2salhd] and the corresponding nickel(II) complex *N,N'*-1,2-*cis*-cyclohexane-1,2-diyl-bis(2-hydroxyacetophenonylideneiminate)nickel(II), [Ni(α,α'-Me_2salhd)], were prepared by a similar procedure.

X-ray quality crystals of [Ni(α,α'-Me_2salen)] and [Ni(3,5-Cl_2saloph)] were obtained by slow cooling of methanolic or ethanolic solutions of the corresponding complex, and those of [Ni(α,α'-Me_2salhd)] by evaporation of acetonitrile solutions.

Electrochemical measurements were performed in dimethyl sulfoxide (Merck, pro analisy); tetra-n-butylammonium perchlorate (TBAP) was prepared and purified by published methods [10].

Physical measurements

NMR spectra were recorded on a Bruker AC 200 spectrometer at 25 °C using tetramethylsilane as internal reference; electronic spectra were recorded at room temperature with a Cary 17DX spectrophotometer.

Electrochemical measurements were made with a potentiostat/galvanostat Princeton Applied Research 273 A, using solutions *c.* 1 mM in complex and 0.1 M in TBAP. Cyclic voltammetry was performed in $(CH_3)_2SO$, in the range −2.5 to 1.5 V, with a platinum microsphere as a working electrode, a platinum wire as a counter electrode, and an Ag/AgCl (1 M NaCl) as reference electrode. In all cases, ferrocene was used as an internal standard. All potentials are reported relative to Ag/AgCl (1 M NaCl) reference electrode and to $E_{1/2}$ of the ferrocenium/ferrocene (Fc^+/Fc); under the experimental conditions used (scan rate 50 mV s^{-1}) the $E_{1/2}$ of the Fc^+/Fc couple is 480 mV in $(CH_3)_2SO$ and ΔE for Fc^+/Fc is 70 mV. The measured potentials were not corrected for junction potentials.

Electrolysis was carried out at controlled potential in a three electrode cell, using a platinum gauze electrode, a platinum foil counter electrode, and Ag/AgCl (1 M NaCl) reference electrode. Electrochemical reduction of [Ni(α,α'-Me_2salen)] and of [Ni(α,α'-Me_2salhd)] was performed at potentials about 100 mV more negative than the cathodic peak potential, whereas electrolysis of [Ni(3,5-Cl_2saloph)] was carried out at the more negative peak potential. Electrochemical oxidation of [Ni(α,α'-Me_2salhd)] was performed at the E_{pa} values (see 'Results and discussion'); the results for the other two complexes were published elsewhere [2, 3].

EPR spectra were obtained with a X-band Varian E 109 spectrometer (9 GHz) equipped with a variable-temperature accessory. Spectra were calibrated with diphenylpicrylhydrazyl (dpph; $g = 2.0037$); the magnetic field was calibrated by use of Mn^{2+} in MgO. Spectra were recorded at −140 °C using sealed quartz tubes and the reported EPR parameters were obtained by computer simulation, in the usual manner [11].

Crystallography

Data collection

For complexes [Ni(3,5-Cl_2saloph)] and [Ni(α,α'-Me_2salen)] intensity data were collected on an Enraf-Nonius CAD 4 diffractometer with graphite monochromatized radiation. The data were empirically cor-

rected for absorption, Lorentz and polarization effects with the CAD 4 software.

Intensity data for [Ni(α,α'-Me_2salhd)] were collected on a FAST area detector diffractometer equipped with a FR 571 rotating anode generator, operating at 3.0 kW, with graphite monochromatized radiation. A crystal to detector distance of 40 mm and a swing angle of $\theta = 25°$ were used; the exposure time was 20 s per frame and an increment between frames of 0.4° was employed. At $\chi = 0°$, one 100° ω scan was done, followed by a second 100° scan at 90° on ϕ. The missing data were then measured by making two further scans at $\chi = 60$ and 135°. Data were evaluated on-line using the modified MADNES [12] software for small molecules, SADNES. With this procedure, a total of 17538 reflections was measured, which reduced to 5075, with an R_{merge} of 0.065. The initial values of the unit cell parameters were determined by an autoindexing procedure applied to 50 intense reflections covering two narrow (*c.* 5° wide) and nearly orthogonal regions of reciprocal space. Throughout data collection, the cell parameters were refined together with the orientation matrix, every 9° of measured data. The values used in the structure determination and refinement are the mean and the corresponding standard deviations were calculated from the refined values of the cell parameters based on more than 200 intense reflections. Data reduction including Lorentz and polarization corrections was carried out by the Kabsh profile fitting method using the program PROCOR [13]. Crystallographic data for all complexes are summarized in Table 1.

Structure solution and refinement

The three structures were solved with a combination of direct methods and Patterson synthesis, using programs SHELX-76 [14] and SHELX-86 [15], and subsequent difference Fourier calculations using SHELX-76. Least-squares refinement was initially done with all non-hydrogen atoms refining isotropically and was then continued assigning to these atoms anisotropic thermal parameters and allowing convergence of the refinement to be achieved.

The hydrogen atoms in the structure of [Ni(3,5-Cl_2saloph)] were located in difference maps, and their positions were introduced and refined isotropically with individual thermal parameters. For the complexes [Ni(α,α'-Me_2salen)] and [Ni(α,α'-Me_2salhd)] the hydrogen positions were calculated and introduced in the refinement with common temperature factors for atoms in similar geometries, namely of type CH, CH_2 and CH_3. In the structure of [Ni(α,α'-Me_2salhd)] a well defined solvent water molecule was found; for [Ni(α,α'-Me_2salen)], a solvent methanol molecule was also found and was refined isotropically.

The final atomic coordinates are given in Tables 2, 3 and 4 for complexes [Ni(α,α'-Me_2salen)], [Ni(α,α'-Me_2salhd)] and [Ni(3,5-Cl_2saloph)], respectively. Drawings were made with the program ORTEP-II [16]. Atomic scattering values were taken from the International Tables [17]. See also 'Supplementary material'.

Results and discussion

Spectroscopic characterization

Nickel(II) complexes with the ligands 3,5-Cl_2saloph and α,α'-Me_2salen have been described elsewhere [2, 3]. Electronic spectra of [Ni(α,α'-Me_2salhd)] in Nujol and in $(CH_3)_2SO$ are almost identical, implying the same structure in solid and solution states. They are very similar to those of the other two low spin square planar Ni(II) complexes reported and of other Ni(II) complexes with pseudomacrocyclic ligands with a N_2O_2 coordination sphere [2, 3, 18, 19]. They exhibit low intensity d–d bands ($\lambda \approx 530$ nm, $\epsilon \approx 120$ M^{-1} cm^{-1}) assigned to transitions from the four low-lying orbitals, that have similar energy, to the empty d_{xy} orbital, that are partially superimposed on a group of high intensity charge transfer bands at higher energies ($\lambda < 440$ nm, $\epsilon \approx 5100$ M^{-1} cm^{-1}).

Molecular structure

In Figs. 1, 2 and 3 are depicted the molecular structures of [Ni(α,α'-Me_2salen)], [Ni(α,α'-Me_2salhd)] and [Ni(3,5-Cl_2saloph)], respectively; their relevant bond lengths and bond angles are listed in Table 5. A complete description of these parameters can be found in Tables S7, S8 and S9, see 'Supplementary material'. In Table S10 are listed maximum deviations from the more important least-square planes in each molecule, as well as angles between planes and lines. These values were calculated to provide a measure of the overall configuration of the three molecules and to simplify and rationalize a comparison between them and with other similar nickel(II) Schiff base complexes.

The coordination geometry around the nickel atom is of type N_2O_2, with the ligands coordinating through the nitrogen and oxygen atoms in *cis* configuration arrangements. The coordinated atoms are almost planar in the structures of [Ni(3,5-Cl_2saloph)] and [Ni(α,α'-Me_2salen)], with maximum deviations from planarity of 0.039(4) and 0.033(6) Å, and the metal atom is, respectively, 0.0078(9) and 0.0073(14) Å away from the coordination planes. The [Ni(α,α'-Me_2salhd)] molecule has a less planar central N_2O_2 unit, with the four atoms distorted in a tetrahedral fashion, with maximum deviations from planarity of 0.076(11) Å and the Ni atom 0.018(2) Å out of that plane.

TABLE 1. Crystallographic and data collection parameters for the complexes studied

	[Ni(α,α'-Me_2salen)]	[Ni(α,α'-Me_2salhd)]	[Ni(3,5-Cl_2saloph)]
Formula	$C_{18}H_{18}N_2O_2Ni$	$C_{22}H_{24}N_2O_2Ni$	$C_{20}H_{10}N_2O_2Cl_4Ni$
Molecular weight	353.04	407.14	510.86
Crystal system	monoclinic	monoclinic	monoclinic
Space group	$C2/c$	$P2_1/a$	$P2_1/n$
Unit cell determination	25 automatically centered reflections with $16 \leqslant \theta \leqslant 18°$		25 automatically centered reflections with $7 \leqslant \theta \leqslant 14°$
a (Å)	25.963(3)	9.645(6)	13.372(5)
b (Å)	7.2973(4)	19.149(16)	8.785(2)
c (Å)	17.357(2)	10.743(5)	16.534(5)
β (°)	107.085(5)	94.66(2)	101.60(3)
V (Å^3)	3143.3	1977.6	1902.7
Z	8	4	4
D_c (g cm^{-3})	1.49	1.37	1.78
μ(Mo Kα) (cm^{-1})	11.76	9.74	8.71
Diffractometer	CAD4	FAST	CAD4
Radiation	Mo Kα ($\lambda = 0.71069$ Å)	Mo Kα	Mo Kα
Scan range (°)	$1.5 \leqslant \theta \leqslant 24$		$1.5 \leqslant \theta \leqslant 28.0$
Scan type	ω–2θ		ω–2θ
No. unique reflexions	2122	4772	3758
No. reflexions with $F \geqslant x\sigma(F)$	1785 ($x = 4$)	1343 ($x = 2$)	2621 ($x = 3$)
Largest peak in final difference Fourier (e/Å^3)	0.47	0.74	0.56
R[a]	0.061	0.085	0.054
R_w[b]			0.044
No. parameters	215	257	302
Weighting scheme	unit	unit	$[2.023/\sigma^2(F) + 0.0002(F)^2]$

[a] $R = \Sigma(F_o - F_c)/\Sigma F_o$. [b] $R_w = \Sigma(F_o - F_c)w^{1/2}/\Sigma(F_o w^{1/2})$.

The molecule of [Ni(3,5-Cl_2saloph)] is virtually planar with a maximum deviation of 0.174(2) Å from a least-squares plane defined by all atoms in the molecule, and 0.129(6) Å when the chlorine atoms are not included in the definition of the molecular plane; in this latter case the chlorine atoms are at a maximum distance of 0.260(2) Å out of that plane.

The molecule of [Ni(α,α'-Me_2salen)] has a stepped configuration as can be seen in Fig. S1. The two six-membered metallocycle rings, NiNCCCO (planes C and G) are almost coplanar, but each makes, however, a significant angle with the benzene rings attached to each of them. The central part of the molecule is quite planar and there is almost no bend at the N...O lines on each side of the molecule. Atoms C(3) and C(4) on the ethylenediamine bridge deviate −0.13(1) and 0.15(1) Å, respectively, from the central NiN_2O_2 plane and the torsion angle N(1)–C(3)–C(4)–N(2) is −23.6(9)°, giving a *cis* conformation to that bridge.

The [Ni(α,α'-Me_2salhd)] molecule is quite distorted, as can be seen in Fig. 2 and judged by the values in Table S10. The steric requirements imposed by interactions between the hydrogens of the cyclohexane ring and those of the aldehyde moieties are such that the two planes defined by the coordinating ring atoms on each side of the molecule, NCCCO, make a considerable dihedral angle, 48.9(5)°, although each side is reasonably planar and is not bent too much at the N...O lines. The bridging atoms, C(3) and C(4), are both on the same side of the NiN_2O_2 plane, deviated 0.15(2) and 0.84(2) Å respectively from it. The torsion about N(1)–C(3)–C(4)–N(2) is 41.8(1.4)° defining a *gauche* conformation for that bridge. The cyclohexane ring adopts a chair conformation with the two methine hydrogen atoms in a *cis* conformation, and since the complex crystallizes in a centric space group both *R,S* and *S,R* enantiomers are present in the crystal.

The Ni–N and Ni–O bonding distances are comparable to the corresponding values observed in similar complexes with the same type of coordination sphere [18, 20–25]. An interesting point concerns the relative magnitudes of Ni–O and Ni–N bond distances. For complexes with ligands where the diimine bridge is aromatic or has three aliphatic carbons the Ni–N distances are longer than the Ni–O distances, whereas for those with two aliphatic carbons the reverse is observed [18, 20–25]. The bond lengths in [Ni(3,5-Cl_2saloph)] have the expected behavior, but [Ni(α,α'-Me_2salen)] and [Ni(α,α'-Me_2salhd)] do not fit the above pattern. The steric strain caused by the non-aromatic cyclic bridge in [Ni(α,α'-Me_2salhd)] with the methyl groups of the aldehyde moiety induces great changes

TABLE 2. Fractional atomic coordinates ($\times 10^4$) for [Ni(α,α'-Me_2salen)]

	x	y	z
Ni	86.4(3)	2396.3(14)	198.3(4)
O(1)	−386(2)	3173(7)	728(2)
O(2)	519(2)	1921(8)	1217(3)
N(1)	−388(2)	2857(8)	−815(3)
N(2)	603(2)	1674(8)	−289(3)
C(1)	−878(3)	3415(10)	−1009(4)
C(11)	−888(3)	3620(10)	423(4)
C(16)	−1166(3)	3711(10)	−404(4)
C(15)	−1720(3)	4103(13)	−642(5)
C(14)	−1987(4)	4440(17)	−88(6)
C(13)	−1714(3)	4437(13)	720(6)
C(12)	−1176(3)	4072(12)	978(5)
C(222)	−1186(3)	3831(13)	−1883(4)
C(3)	−117(3)	2623(14)	−1449(4)
C(2)	1100(3)	1208(10)	49(4)
C(21)	1025(3)	1465(10)	1446(4)
C(26)	1342(3)	1160(10)	925(4)
C(25)	1893(3)	766(14)	1271(5)
C(24)	2121(3)	646(17)	2082(6)
C(23)	1802(4)	900(13)	2585(5)
C(22)	1266(3)	1261(11)	2286(4)
C(111)	1459(3)	653(14)	−476(5)
C(4)	380(3)	1577(12)	−1175(4)
O(3)	0	6417(20)	7500
C(30)	0	−1593(58)	7500

TABLE 3. Fractional atomic coordinates ($\times 10^4$) for [Ni(α,α'-Me_2salhd)]

	x	y	z
Ni	2244(2)	2060(1)	274(2)
O(1)	3073(10)	1321(5)	1104(11)
O(2)	2266(11)	1519(5)	−1162(10)
N(1)	2041(11)	2572(6)	1710(12)
N(2)	1497(11)	2824(6)	−612(12)
C(11)	3052(14)	1182(9)	2306(17)
C(12)	3654(15)	548(9)	2721(19)
C(13)	3579(19)	330(9)	3905(20)
C(14)	2961(18)	741(10)	4748(19)
C(15)	2377(16)	1371(10)	4377(16)
C(16)	2405(14)	1623(8)	3141(16)
C(21)	1243(18)	1561(10)	−2007(16)
C(22)	829(19)	927(10)	−2655(16)
C(23)	−244(19)	922(11)	−3533(17)
C(24)	−986(19)	1536(12)	−3848(18)
C(25)	−626(17)	2135(11)	−3288(14)
C(26)	475(16)	2180(9)	−2374(14)
C(1)	1857(14)	2301(8)	2809(16)
C(2)	864(14)	2834(9)	−1714(15)
C(3)	1658(15)	3307(8)	1442(15)
C(4)	1996(16)	3486(9)	91(14)
C(5)	3518(16)	3581(9)	−150(18)
C(6)	4132(18)	4128(9)	772(23)
C(7)	3941(20)	3909(10)	2103(21)
C(8)	2407(16)	3841(9)	2300(16)
C(111)	480(18)	3505(8)	−2370(16)
C(222)	1024(16)	2673(9)	3729(15)
O(w)	8862(14)	4691(7)	−667(14)

in the geometry of the molecule and the balance between tetrahedral/square planar geometry will induce great distortion, as to make meaningless any attempt to rationalize small differences in bond lengths. For [Ni(α,α'-Me_2salen)], a molecule with two aliphatic carbons in the bridge, the Ni–N are usually longer than Ni–O bond lengths, a situation that must be contrasted with that of [Ni(salen)] [21]. We also attribute this anomalous behavior to steric strain, in this case between the methyl groups in the aldehyde moiety and the hydrogens of the ethylene bridge, although less severe than in [Ni(α,α'-Me_2salhd)]. Two possibilities could be envisioned to relieve strain: an increase in the torsion angle N(1)–C(3)–C(4)–N(2), but at the expense of equatorial ligand planarity; or a reduction of the torsion angle, accompanied by an increase of the bite of the bridging nitrogen atoms that must be accompanied by an increase in Ni–N bond lengths. The latter model must be operative in [Ni(α,α'-Me_2salen)] as: (i) its torsion angle, −23.6(9)°, is smaller than the value of −34.0(3)° observed in [Ni(salen)] [21]; and (ii) its bond lengths are longer than those of this latter complex, for which Ni–N distances of 1.853 and 1.834 Å were reported [21].

Crystal packing

The crystal packing of [Ni(3,5-Cl_2saloph)] and [Ni(α,α'-Me_2salen)] involves the pairing of two centrosymmetrically related molecules in dimers, as observed in many other similar structures [21, 23]. The Ni...Ni distance in these dimers is 3.582(1) Å in [Ni(3,5-Cl_2saloph)] and 3.567(1) Å in [Ni(α,α'-Me_2salen)]. The Ni...Ni vector makes a more acute angle with the NiN_2O_2 plane in [Ni(3,5-Cl_2saloph)], 76.23(7)°, than in [Ni(α,α'-Me_2salen)], 81.38(13)°, corresponding to a greater shift, in the first case, of the two molecules in the dimer relative to each other. The packing of [Ni(α,α'-Me_2salhd)] with no systematic parallel orientation of any part of the complex molecules shows no similarity with any of these types of arrangements. The steric requirements and the geometry of the cyclohexane ring relative to the aldehyde moieties impose a packing with the shortest distance between two Ni atoms, Ni...Ni ($-0.5+x$, $0.5-y$, z), of 5.108(3) Å. To our knowledge, there is no other known structure of a nickel(II) complex with a Schiff base possessing an N_2O_2 coordination sphere and with a cycloalkane ring linking the two aldehyde moieties as in [Ni(α,α'-Me_2salhd)]. The only other example of a complex with folded molecules is [Ni(nappd)] [22], where the two halves of the molecule are related by a crystallographic mirror plane and fold at the nickel atom, forming a angle between the two metallocycle planes of 37.0(1)°.

TABLE 4. Fractional atomic coordinates ($\times 10^4$) for [Ni(3,5-Cl_2saloph)]

	x	y	z
Ni	69.0(5)	1938.8(7)	342.0(4)
O(1)	956(2)	851(4)	1128(2)
O(2)	1240(2)	2650(4)	37(2)
N(1)	−1103(3)	1169(5)	637(2)
N(2)	−806(3)	3115(5)	−424(2)
Cl(1)	116(1)	−3591(2)	3545(1)
Cl(2)	2772(1)	−484(2)	2130(1)
Cl(21)	1734(1)	6938(2)	−2557(1)
Cl(22)	3320(1)	2929(2)	−186(1)
C(1)	−1136(4)	207(6)	1217(3)
C(2)	−553(4)	4086(6)	−936(3)
C(3)	−2019(4)	1794(6)	162(3)
C(4)	−1852(4)	2897(6)	−403(3)
C(5)	−2669(4)	3661(7)	−874(3)
C(6)	−3651(5)	3290(9)	−799(4)
C(7)	−3812(5)	2200(8)	−257(4)
C(8)	−3004(5)	1441(7)	231(4)
C(11)	728(4)	−95(5)	1664(3)
C(12)	1520(4)	−854(6)	2220(3)
C(13)	1345(4)	−1861(6)	2803(3)
C(14)	348(4)	−2201(6)	2854(3)
C(15)	−444(4)	−1517(6)	2345(3)
C(16)	−274(4)	−462(5)	1746(3)
C(21)	1309(4)	3576(5)	−554(3)
C(22)	2276(4)	3882(6)	−746(3)
C(23)	2403(4)	4886(6)	−1340(3)
C(24)	1569(4)	5651(6)	−1797(3)
C(25)	620(4)	5403(6)	−1646(3)
C(26)	469(4)	4359(6)	−1035(3)

However and in spite of this bent form, the molecules pack in the unit cell of this structure on top of each other, forming an infinite Ni...Ni...Ni chain along the *c* axis. In Figs. S1, S2 and S3 packing diagrams of the three crystal structures are represented in an orientation to show a side view of each molecule.

Electrochemistry and EPR characterization of electrolyzed solutions

Reduction

Cyclic voltammograms of [Ni(α,α'-Me_2salen)] and [Ni(α,α'-Me_2salhd)] show a single reduction process characteristic of diffusion-controlled reversible one-electron charge transfer, as supported by equal anodic and cathodic current, anodic–cathodic peak potential separation ≈ 70 mV ($\Delta E(Fc^+/Fc) = 70$ mV), and linear dependence between i_p and $v^{1/2}$ for the scan rates studied (20 to 500 mV s^{-1}) [26]. Electrochemical data are summarized in Table 6 and in Fig. 4 are depicted cyclic voltammograms of [Ni(α,α'-Me_2salen)] in $(CH_3)_2SO$ at several scan rates.

Reductive behavior of [Ni(3,5-Cl_2saloph)] is more complex, since the number of waves observed depends on the scan range used. On scanning from 0 V to −2.5 V cyclic voltammograms show three poorly resolved waves on the cathodic scan, and on the reverse sweep besides three poorly resolved anodic peaks related with the cathodic waves, two more well separated waves are observed. The proximity of the three waves hampered the electrochemical characterization of each individual charge transfer process. However, when the positive potential limit is increased to 1.0 V, two more waves can be observed: one in the cathodic and the other in the anodic scan; these new bands appear to relate to a common electron transfer process (Fig. 5).

Electrochemical reductions of [Ni(α,α'-Me_2salen)] and [Ni(α,α'-Me_2salhd)] produce a color change of their $(CH_3)_2SO$ solutions from reddish to dark green, implying the formation of new species. Frozen solution

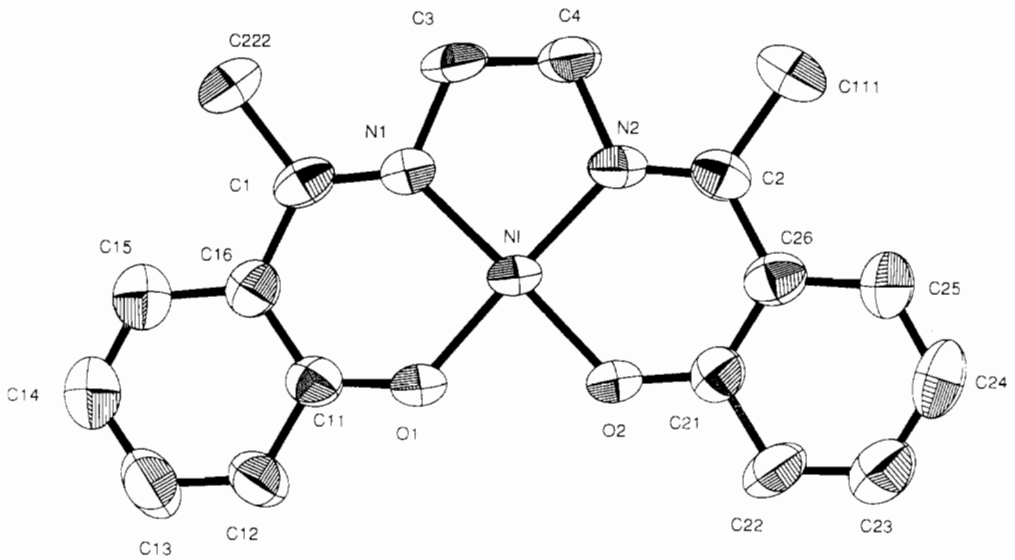

Fig. 1. ORTEP diagram of [Ni(α,α'-Me_2salen)] showing 50% thermal ellipsoids.

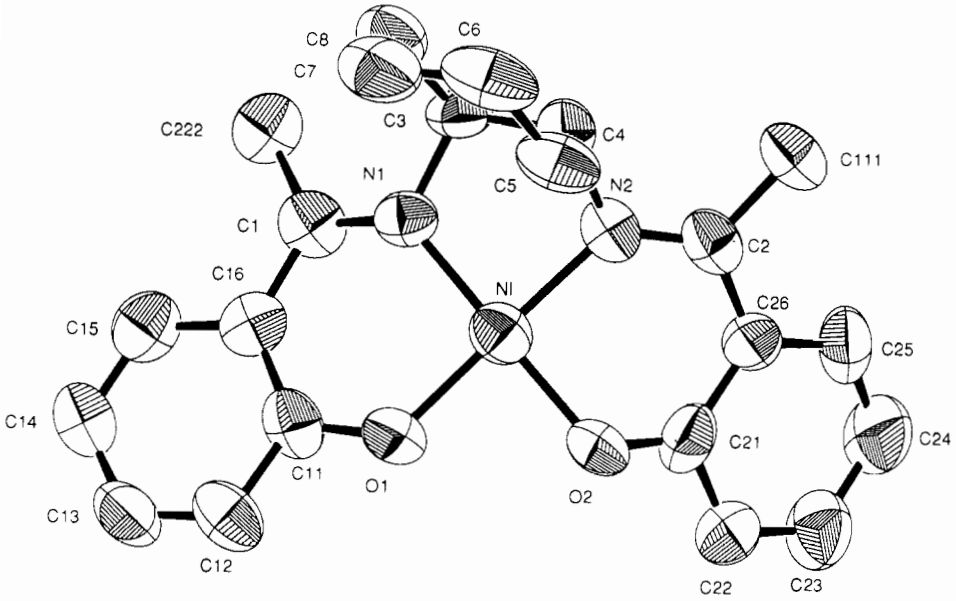

Fig. 2. ORTEP diagram of [Ni(α,α'-Me_2salhd)] showing 50% thermal ellipsoids.

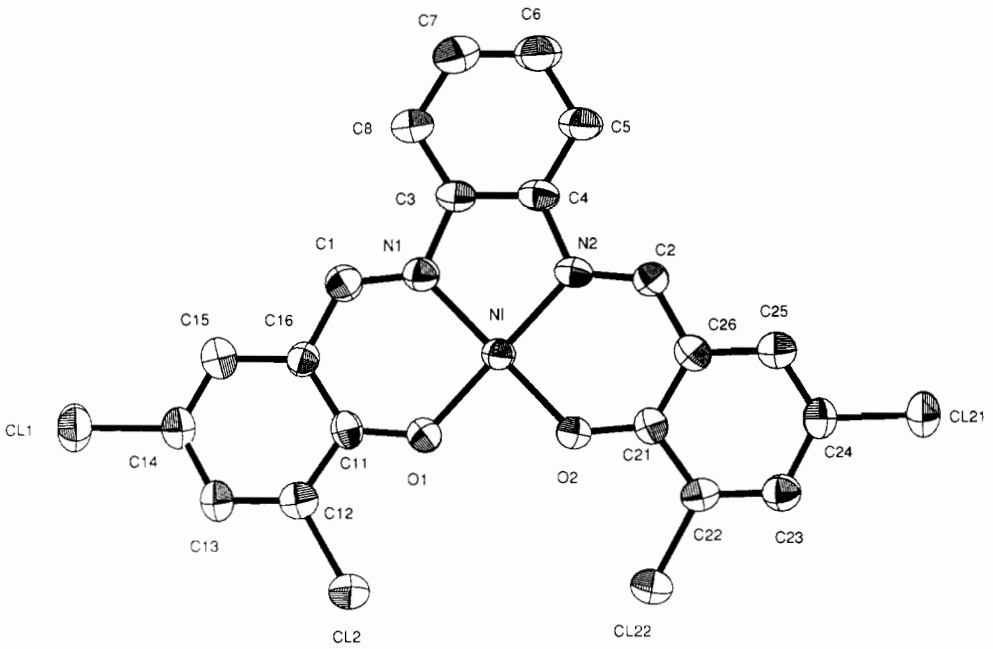

Fig. 3. ORTEP diagram of [Ni(3,5-Cl_2saloph)] showing 50% thermal ellipsoids.

EPR spectra of electrochemically generated species are very similar and show rhombic symmetry, large g tensor anisotropy and hyperfine splittings (quintuplet) in the low g region. These results imply a metal-centered reduction process, and the electrochemically reduced species must be associated with Ni(I) complexes. The presence of a quintuplet in the high magnetic field region is consistent with interaction of the unpaired electron with the two nitrogen atoms (^{14}N; $I=1$) of the equatorial ligand (Fig. 6). The observed coupling constants ($A(N)=0.9$ mT) are very similar to those reported for Ni(I) complexes with tetraaza and porphyrinic macrocyclic ligands [4, 27, 28]. In the absence of EPR crystal data for these complexes, the observed similarity between their g features/$A(N)$ values with those of (i) Ni(I) complexes with tetraaza macrocyclic ligands and (ii) analogous isoelectronic d^9 Cu(II) complexes, can be taken as support for the following orientation scheme for tensor axes in our nickel complexes: $g_1=g_z$; $g_2=g_x$; $g_3=g_y$ where g_1 and g_3 refer to the lowest

TABLE 5. Relevant bond lengths (Å) and bond angles (°) for the complexes studied

[Ni(α,α′-Me$_2$salen)]		[Ni(α,α′-Me$_2$salhd)]		[Ni(3,5-Cl$_2$saloph)]	
Bond lengths					
Ni–O(1)	1.827(5)	Ni–O(1)	1.823(12)	Ni–O(1)	1.841(5)
Ni–O(2)	1.829(5)	Ni–O(2)	1.860(13)	Ni–O(2)	1.847(5)
Ni–N(1)	1.858(5)	Ni–N(1)	1.851(14)	Ni–N(1)	1.859(6)
Ni–N(2)	1.862(6)	Ni–N(2)	1.858(13)	Ni–N(2)	1.856(6)
O(1)–C(11)	1.298(8)	C(11)–O(1)	1.319(19)	C(11)–O(1)	1.294(6)
O(2)–C(21)	1.300(8)	C(21)–O(2)	1.288(19)	C(21)–O(2)	1.290(6)
N(1)–C(1)	1.284(8)	C(1)–N(1)	1.315(18)	C(1)–N(1)	1.285(7)
N(1)–C(3)	1.481(8)	C(3)–N(1)	1.477(18)	C(2)–N(2)	1.294(7)
N(2)–C(2)	1.297(9)	C(2)–N(2)	1.288(18)	C(3)–N(1)	1.426(7)
N(2)–C(4)	1.477(8)	C(4)–N(2)	1.532(20)	C(4)–N(2)	1.419(7)
C(1)–C(16)	1.471(1)	C(16)–C(11)	1.414(21)	C(16)–C(1)	1.427(8)
C(1)–C(222)	1.524(9)	C(1)–C(16)	1.435(21)	C(26)–C(2)	1.429(8)
C(11)–C(16)	1.407(9)	C(26)–C(21)	1.436(22)	C(4)–C(3)	1.394(8)
C(3)–C(4)	1.45(1)	C(2)–C(26)	1.473(21)	C(16)–C(11)	1.411(7)
C(2)–C(26)	1.465(9)	C(222)–C(1)	1.502(21)	C(26)–C(21)	1.417(7)
C(2)–C(111)	1.54(1)	C(111)–C(2)	1.498(20)		
C(21)–C(26)	1.41(1)	C(4)–C(3)	1.552(22)		
Bond angles					
O(2)–Ni–O(1)	83.3(2)	O(2)–Ni–O(1)	86.5(5)	O(2)–Ni–O(1)	84.7(2)
N(1)–Ni–O(1)	93.7(2)	N(1)–Ni–O(1)	94.3(6)	N(1)–Ni–O(1)	94.8(3)
N(1)–Ni–O(2)	176.7(2)	N(1)–Ni–O(2)	174.4(5)	N(1)–Ni–O(2)	178.4(2)
N(2)–Ni–O(1)	176.3(2)	N(2)–Ni–O(1)	176.7(5)	N(2)–Ni–O(1)	177.4(2)
N(2)–Ni–O(2)	93.8(2)	N(2)–Ni–O(2)	92.5(6)	N(2)–Ni–O(2)	94.5(3)
N(2)–Ni–N(1)	89.2(2)	N(2)–Ni–N(1)	87.0(6)	N(2)–Ni–N(1)	86.1(3)
C(11)–O(1)–Ni	128.1(4)	C(11)–O(1)–Ni	126.5(11)	C(11)–O(1)–Ni	127.6(4)
C(21)–O(2)–Ni	128.5(4)	C(21)–O(2)–Ni	119.4(11)	C(21)–O(2)–Ni	127.9(4)
C(1)–N(1)–Ni	129.4(5)	C(1)–N(1)–Ni	124.8(12)	C(1)–N(1)–Ni	126.3(5)
C(3)–N(1)–Ni	110.9(4)	C(3)–N(1)–Ni	112.5(11)	C(3)–N(1)–Ni	113.0(4)
C(3)–N(1)–C(1)	119.6(6)	C(3)–N(1)–C(1)	120.0(14)	C(3)–N(1)–C(1)	120.6(5)
C(2)–N(2)–Ni	128.6(5)	C(2)–N(2)–Ni	128.1(12)	C(2)–N(2)–Ni	127.0(4)
C(4)–N(2)–Ni	111.9(4)	C(4)–N(2)–Ni	107.8(10)	C(4)–N(2)–Ni	113.4(4)
C(4)–N(2)–C(2)	119.5(6)	C(4)–N(2)–C(2)	123.2(13)	C(4)–N(2)–C(2)	119.6(5)
C(16)–C(1)–N(1)	122.2(6)	C(16)–C(11)–O(1)	122.9(16)	C(16)–C(1)–N(1)	125.7(6)
C(222)–C(1)–N(1)	120.9(7)	C(1)–C(16)–C(11)	123.7(16)	C(26)–C(2)–N(2)	124.6(6)
C(222)–C(1)–C(16)	116.9(6)	C(26)–C(21)–O(2)	126.3(17)	C(4)–C(3)–N(1)	113.7(5)
C(16)–C(11)–O(1)	125.4(6)	C(2)–C(26)–C(21)	117.7(15)	C(3)–C(4)–N(2)	113.6(5)
C(11)–C(16)–C(1)	120.4(6)	C(16)–C(1)–N(1)	120.4(15)	C(16)–C(11)–O(1)	124.8(5)
C(4)–C(3)–N(1)	112.8(6)	C(222)–C(1)–N(1)	121.5(15)	C(11)–C(16)–C(1)	120.9(6)
C(26)–C(2)–N(2)	122.8(6)	C(222)–C(1)–C(16)	118.1(16)	C(26)–C(21)–O(2)	124.2(5)
C(111)–C(2)–N(2)	119.7(7)	C(26)–C(2)–N(2)	120.9(15)	C(21)–C(26)–C(2)	121.5(5)
C(111)–C(2)–C(26)	117.5(7)	C(111)–C(2)–N(2)	121.7(16)		
C(26)–C(21)–O(2)	125.0(7)	C(111)–C(2)–C(26)	117.4(15)		
C(21)–C(26)–C(2)	120.7(7)	C(4)–C(3)–N(1)	108.9(13)		
C(3)–C(4)–N(2)	110.7(6)	C(3)–C(4)–N(2)	101.3(13)		

TABLE 6. Electrochemical data for reduction of Ni(II) complexes in $(CH_3)_2SO$ (0.1 M TBAP)[a]

Complex	Ag/AgCl (1 M NaCl)				Fc^+/Fc	
	E_{pa}	E_{pc}	ΔE	$E_{1/2}$	$E_{1/2}$	i_{pc}/i_{pa}[b]
[Ni(α,α′-Me$_2$salen)]	−1665	−1735	79	−1700	−2180	1.1
[Ni(α,α′-Me$_2$salhd)]	−1630	−1695	65	−1663	−2143	1.1

[a]All potentials in mV. Solute concentration $\approx 10^{-3}$ M; $\Delta E = E_{pa} - E_{pc}$; $E_{1/2} = \frac{1}{2}(E_{pa} + E_{pc})$; and E_{pa} and E_{pc} are the anodic and cathodic peak potential, respectively; scan rate = 50 mV/s. Under the conditions used, $E_{1/2}$ (Fc^+/Fc) is 480 mV. [b]The ratio i_{pc}/i_{pa} is constant for scan rates in the range 20–500 mV/s.

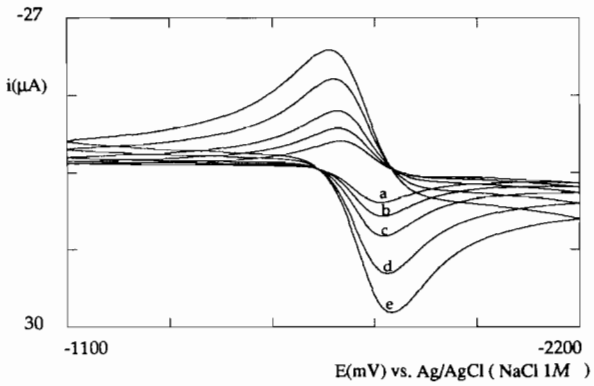

Fig. 4. Variable scan rate cyclic voltammograms of [Ni(α,α'-Me_2salen)] in $(CH_3)_2SO$/0.1 M TBAP; potentials reported vs. Ag/AgCl (1 M NaCl); scan rate in mV/s: (a) 20; (b) 50; (c) 100; (d) 200; (e) 500.

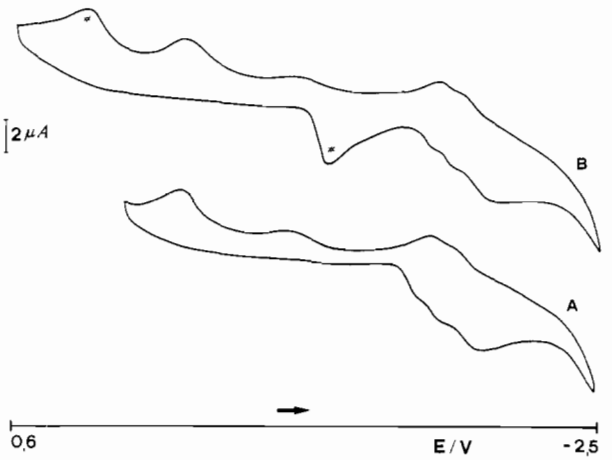

Fig. 5. Cyclic voltammograms of the reduction process of [Ni(3,5-Cl_2saloph)] in $(CH_3)_2SO$/0.1 M TBAP; potentials reported vs. Ag/AgCl (1 M NaCl); scan rate = 50 mV/s; (A) from 0 to −2.5 V, (B) from +0.6 to −2.5 V. The additional peaks in (B) relate to a new redox process; see text for details.

and highest magnetic field g values, respectively. Furthermore, based on the above discussion, a d_{xy}^1 ground state is assumed since $g_z > g_x$; g_y [4, 29]. EPR data for the complexes are summarized in Table 7.

The fact that addition of a large excess of pyridine to the electrolyzed solutions does not alter their EPR spectra also suggests that the nickel(I) species exist as tetracoordinate complexes and thus can be formulated as [Ni(α,α'-Me_2salen)]$^-$ and [Ni(α,α'-Me_2salhd)]$^-$.

Electrochemical reduction of [Ni(3,5-Cl_2saloph)] also produces a color change of its $(CH_3)_2SO$ solutions, but from reddish to dark brown, suggesting the presence in solution of new electrolyzed species, that should be different from those of the complexes discussed above. Frozen solution EPR spectra of the electrochemically reduced solutions are in fact very different from the EPR spectra of Ni(α,α'-Me_2salen)]$^-$ and [Ni(α,α'-Me_2salhd)]$^-$. They show only a low intensity pseudo-isotopic signal with a g value very close to that of the free electron, which is indicative of a ligand-centered reduction process. The observed low intensity signal may imply subsequent fast reaction of the anion radical of the nickel(II) complex to give diamagnetic dimers, as has been demonstrated for nickel(II) complexes with very similar Schiff base ligands [30]. It was not possible, under the experimental conditions employed, to observe EPR signals characteristic of Ni(I) species, which suggests (i) fast decomposition of the generated Ni(I) complexes to prevent preparative scale electrolysis, or (ii) that the potential necessary to reduce the metal center is more negative than those used in this work.

In order to obtain additional support for any of these hypotheses, we attempted to chemically reduce nickel(II) solutions of this complex, using a strong reducing agent, sodium amalgam, hoping that (i) a shorter reaction time would allow observation of the unstable species, and (ii) that the potential of the reductant could be negative enough (−2.05 V versus SCE in acetonitrile and in tetrahydrofuran [31]) to reduce the metal center. However, only the low intensity EPR signal due to radical species could be detected, and thus none of the hypotheses could be ruled out. No spectroscopic characterization of the anion radical Ni(II) species obtained under the experimental conditions used was pursued.

Oxidation

The oxidative behavior of [Ni(α,α'-Me_2salen)] and [Ni(3,5-Cl_2saloph)] in $(CH_3)_2SO$ has been described elsewhere [2, 3], and the cyclic voltammograms show, for the scan rates used (20 to 200 mV/s), one electron reversible oxidation process assigned to Ni(II)/Ni(III) and the beginning of a second irreversible oxidation (ligand-centered oxidation) in the limit of the potential range studied. The cyclic voltammograms of [Ni(α,α'-Me_2salhd)] also show one electron reversible oxidation process (at 50 mV/s: $\Delta E_p = 80$ mV; $i_p/v^{1/2}$ is independent of scan rate; and $i_{pc}/i_{pa} \approx 1$ for the scan rates studied [26]), and the beginning of another anodic wave at the limit of the anodic potential used. Electrochemical data for the oxidation processes are summarized in Table 8.

Electrochemical oxidation of [Ni(α,α'-Me_2salhd)] in $(CH_3)_2SO$, at the E_{pa} value, produces a color change of the solution from reddish to dark brown, implying the formation of new species in solution. Frozen solution EPR spectra of electrolytically generated nickel complexes show the rhombic symmetry and the large g tensor anisotropy that are associated with a metal center oxidation process. The spectra show no hyperfine splittings due to the equatorial nitrogen atoms and are similar to those of electrogenerated [Ni(3,5-

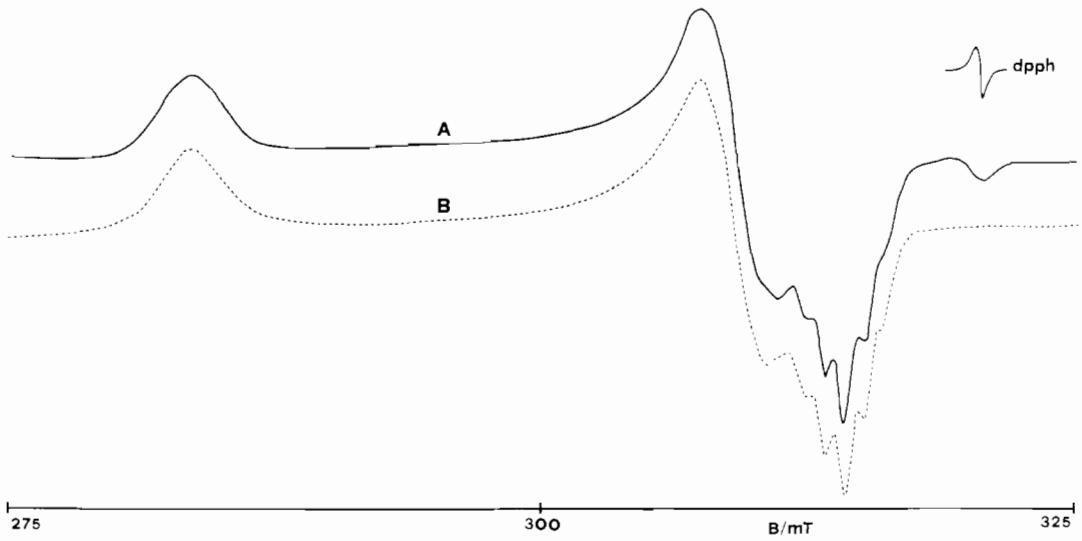

Fig. 6. (A) Frozen solution X-band EPR spectrum of an electrochemically reduced solution of [Ni(α,α'-Me_2salen)] in $(CH_3)_2SO$/0.1 M TBAP, obtained at −120 °C. (B) Computer simulation of (A), using the parameters in Table 10.

TABLE 7. EPR parameters for electrochemically reduced solutions of the complexes studied[a]

Complex	g_z	g_x	g_y	g_{av}[b]	A_z(N) (mT)	A_x(N) (mT)	A_y(N) (mT)
[Ni(3,5-Cl_2saloph)]	[c]						
[Ni(α,α'-Me_2salen)]	2.267	2.078	2.044	2.130	0.77	0.83	0.94
[Ni(α,α'-Me_2salhd)]	2.281	2.075	2.046	2.134	0.80	0.87	0.98

[a]Obtained by computer simulation of the experimental EPR spectra. [b]The value of g_{av} is $1/3(g_x+g_y+g_z)$. [c]EPR spectra typical of a radical species ($g\approx 2.00$).

TABLE 8. Electrochemical data for the oxidation of Ni(II) complexes in 0.1 M TBAP in $(CH_3)_2SO$ and EPR parameters for their electrochemically oxidized solutions[a,b]

Complex	Cyclic voltammetry data						EPR parameters[c]				Reference
	Ag/AgCl (1 M NaCl)				Fc^+/Fc		g_x	g_y	g_z	g_{av}[e]	
	E_{pa}	E_{pc}	ΔE	$E_{1/2}$	$E_{1/2}$	i_{pc}/i_{pa}[d]					
[Ni(3,5-Cl_2saloph)]	938	828	110	883	403	1.0	2.234	2.204	2.020	2.153	2
[N(α,α'-Me_2salen)]	795	685	110	740	260	1.0	2.266	2.220	2.021	2.169	3
[Ni(α,α'-Me_2salhd)]	671	827	78	749	269	1.0	2.270	2.221	2.024	2.172	this work

[a]All potentials in mV. Solute concentration $\approx 10^{-3}$ M; scan rate = 50 mV/s; $\Delta E = E_{pa} - E_{pc}$; $E_{1/2} = \frac{1}{2}(E_{pa}+E_{pc})$; and E_{pa} and E_{pc} are the anodic and cathodic peak potential, respectively. Under the conditions used, $E_{1/2}(Fc^+/Fc)$ is 480 mV. [b]The nickel(III) species in solution are formulated as $[NiL((CH_3)_2SO)_2]^+$, where L is a Schiff base ligand (see text for details). [c]Values obtained by computer simulation and EPR spectra. [d]The ratio i_{pc}/i_{pa} is constant for scan rates in the range 20–100 mV/s. [e]The value of g_{av} is $1/3(g_x+g_y+g_z)$.

Cl_2saloph)$\{(CH_3)_2SO\}_2]^+$ and [Ni(α,α'-Me_2salen)-$\{(CH_3)_2SO\}_2]^+$. These complexes were found to be low spin and elongated along the axial axes, and to possess a $^2A_1(d_{z^2})$ ground state [2, 3]. EPR data for the complexes are summarized in Table 8.

However, when electrolysis was performed at a potential value 100 mV above the E_{pa} value, the resulting solutions exhibit EPR spectra that show the bands typical of Ni(III) complexes but superimposed on a signal centered at $g\approx 2.00$, that has been assigned to radical species formed by oxidation of the coordinated ligand [3, 18].

When excess pyridine is added to electrolyzed solutions of Ni(II) complexes, new frozen solution EPR spectra are detected suggesting the presence of different Ni(III) species in solution. The new spectra also exhibit

rhombic symmetry and g tensor anisotropy ($g_x = 2.203$; $g_y = 2.178$; $g_z = 2.027$), but with hyperfine splittings in the three g regions due to the interaction of the unpaired electron with nitrogen atoms of the two pyridine molecules that are axially coordinated: one well resolved quintuplet ($A(N) = 2.14$ mT) in the high magnetic field region, and two incompletely resolved quintuplets in the two other g regions ($A(N) = 1.82$ mT). The new complex, formulated as $[Ni(\alpha,\alpha'\text{-}Me_2salhd)(py)_2]^+$, has the same $^2A_1(d_{z^2})$ ground state assigned to the other complexes [2, 3] and its rapid formation supports lability for these axial bonds.

Conclusions

Species generated by one-electron electrochemical oxidation/reduction of the nickel(II) complexes reported in this work were characterized by EPR spectroscopy, and the results obtained allow for an unambiguous identification of electron transfer sites. All four-coordinate complexes were oxidized at the metal center with an increase in coordination number through binding of two solvent molecules. Reduction of the same nickel(II) complexes yielded metal-centered reduced species only for those with an aliphatic diimine bridge; for [Ni(3,5-Cl_2saloph)] only ligand reduction was observed.

Our data also suggest that on reduction to Ni(I), the coordination environment of the parent complexes is not changed, a result that must be contrasted with that found for the oxidation of the same nickel(II) complexes, where an increase in coordination number is observed. This is an expected increase, as high oxidation states in nickel complexes require the large ligand field stabilization energies provided by hexacoordination to strong donating ligands. In fact, we have shown that for nickel(II) complexes with this type of N_2O_2 Schiff base ligand, metal-centered oxidation could only be observed in strongly donating solvents or in the presence of good donor molecules, such as pyridine [2, 3].

The invariance on coordination number on reduction, can be accounted for by the known preference of low valent nickel complexes for tetracoordinate geometries in complexes with strong field ligands.

For macrocyclic ligands a number of factors has already been identified that control the oxidation/reduction site and the redox potentials of their nickel(II) complexes: these include chelate ring size/hole size [4, 5], ring ruffling/axial ligation [6, 7], degree and distribution of unsaturation [4, 8], and substitution pattern in the chelate ring [4, 9].

The reduction site depends both upon the relative energies of the d_{xy} metal orbital and of the π^* macrocyclic orbital; furthermore the energy of this latter orbital is lowered when the degree of unsaturation of the ligand is increased [4, 8], and for our complexes becomes lower than that of the metal orbital for [Ni(3,5-Cl_2saloph)], thus making the ligand the preferred site for reduction processes.

Reduction potentials of $[Ni(\alpha,\alpha'\text{-}Me_2salen)]$ and $[Ni(\alpha,\alpha'\text{-}Me_2salhd)]$ show similar values, although slightly more positive for the latter complex, and the larger hole size in $[Ni(\alpha,\alpha'\text{-}Me_2salhd)]$ can be invoked to contribute to the more positive $E_{1/2}$ found for this complex, as it can more easily accommodate the size increase expected with the addition of an antibonding d electron. Although no structural data could be obtained for nickel(I) complexes, the observation that these complexes do not form additional bonds, even in the presence of pyridine, can be taken to imply that formation of reduced complexes must induce some degree of tetrahedral distortion. Nickel(II) complexes that already have tetrahedral distorsions will then be more easily reduced as the structural changes that follow reduction would be minimized. We believe that the lower potential observed for $[Ni(\alpha,\alpha'\text{-}Me_2salhd)]$ must be ascribed to a combination of these two contributions, as this nickel(II) complex has both a large hole size and significant tetrahedral distortion.

Values of $E_{1/2}$ for the oxidation process of the complexes studied show that $[Ni(\alpha,\alpha'\text{-}Me_2salen)]$ is easier to oxidize than $[Ni(\alpha,\alpha'\text{-}Me_2salhd)]$ by 50 mV, where [Ni(3,5-Cl_2saloph)] shows the highest oxidation potential. The difference observed between the oxidation potentials of $[Ni(\alpha,\alpha'\text{-}Me_2salen)]$ and $[Ni(\alpha,\alpha'\text{-}Me_2salhd)]$ contrast with the similarity of $E_{1/2}$ for the reduction processes. Based on the X-ray data obtained for $[Ni(\alpha,\alpha'\text{-}Me_2salhd)]$, this observation is consistent with an interpretation in terms of the presence of steric hindrance for axial binding due to the axially oriented cyclohexane bridge, that prevents the stabilization of Ni(III) by the solvent molecules; furthermore the planarity of the NiN_2O_2 unit in $[Ni(\alpha,\alpha'\text{-}Me_2salen)]$ makes axial coordination easier for this complex and will thus facilitate its oxidation. Finally, we note that as observed for [Ni(3,5-Cl_2saloph)] which has an aromatic diimine bridge, an increase in unsaturation will decrease electron density on the metal through delocalization onto the ligand and so will increase the difficulty to oxidize the metal center.

Supplementary material

The atomic coordinates and thermal parameters for the hydrogen atoms (Tables S1, S3 and S5), anisotropic thermal parameters for all the non-hydrogen atoms (Tables S2, S4 and S6), bond lengths and bond angles

(Tables S7, S8 and S9), equations of least-squares planes, deviations of atoms and angles between planes (Table S10), lists of observed and calculated structure factors, and a stereoscopic view of the unit cell (Figs. S1, S2 and S3) for [Ni(α,α'-Me_2salen)], [Ni(α,α'-Me_2salhd)] and [Ni(3,5-Cl_2saloph)] are available on request from the authors.

Acknowledgements

Partial financial support for this work was provided by JNICT (Lisboa) through contract STRDA/C/CEN/417/92 (to B.C.). F.A. thanks JNICT for a fellowship; M.C. and K.N. were Erasmus students at ICTB (PIC NL-1067).

References

1 J.R. Lancaster (ed.), *The Bioinorganic Chemistry of Nickel*, VCH, New York, 1988.
2 B. de Castro and C. Freire, *Inorg. Chem., 29* (1990) 5113.
3 B. de Castro and C. Freire, *Inorg. Chem.*, submitted for publication.
4 F.V. Lovecchio, E.S. Gore and D.H. Busch, *J. Am. Chem. Soc., 96* (1974) 3104.
5 G.K. Barefield, G.M. Freeman and D.G. Derveer, *Inorg. Chem., 25* (1986) 552.
6 C. Kratky, R. Tshatka, C. Angst, J.E. Johansen, J.C. Plaquevent, J.C. Schreiber and A. Eschenmoser, *Helv. Chim. Acta, 68* (1985) 1312.
7 P.A. Connick and K.A. Macor, *Inorg. Chem., 30* (1991) 4654.
8 A.M. Tait, F.V. Lovecchio and D.H. Busch, *Inorg. Chem., 16* (1977) 2206.
9 J.A. Strecky, D.G. Pillsbury and D.H. Busch, *Inorg. Chem., 19* (1980) 3148.
10 R.J. Blau and J.H. Espenson, *J. Am. Chem. Soc., 108* (1988) 1962.
11 J.R. Pilbrow and M.E. Winfield, *Mol. Phys., 23* (1973) 1073.
12 A. Messerschmidt and J.W. Plugrath, *J. Appl. Crystallogr., 20* (1987) 306.
13 W. Kabsch, *J. Appl. Crystallogr., 21* (1988) 916.
14 G.M. Sheldrick, *SHELX*, crystallography calculation program, University of Cambridge, UK, 1976.
15 G.M. Sheldrick, in G.M. Sheldrick, C. Kruger and R. Goddard (eds.), *Crystallography Computing 3*, Oxford University Press, Oxford, 1985.
16 C.K. Johnson, *ORTEP-II, Rep. ORNL-5138*, Oak Ridge National Laboratory, Oak Ridge, TN, 1976.
17 *International Tables for X-ray Crystallography*, Vol. IV, Kynoch Birmingham, UK, 1974.
18 M.A.A.F. de C.T. Carrondo, B. de Castro, A.M. Coelho, D. Domingues, C. Freire and J. Morais, *Inorg. Chim. Acta, 205* (1993) 157.
19 A.B.P. Lever, *Inorganic Electronic Spectroscopy*, Elsevier, New York, 2nd edn., 1984.
20 A. Rahda, M. Seshasaycc, K. Ramalingam and G. Aravamudan, *Acta Crystallogr., Sect. C, 41* (1985) 1169.
21 A.G. Manfredotti and C. Gusatini, *Acta Crystallogr., Sect. C, 39* (1983) 863.
22 F. Akhatar and M.G.B. Drew, *Acta Crystallogr., Sect. B, 38* (1982) 1149.
23 F. Akhatar, *Acta Crystallogr., Sect. B, 37* (1982) 84.
24 R.P. Scaringe and D.J. Hodgson, *Inorg. Chem., 15* (1976) 1193.
25 M.G.B. Drew, R.N. Prasard and R.P. Sharma, *Acta Crystallogr., Sect. C, 41* (1985) 1755.
26 A.J. Bard and L.R. Faulkner, *Electrochemical Methods—Fundamentals and Applications*, Wiley, New York, 1980.
27 B. Jaun and A. Pfaltz, *J. Chem. Soc., Chem. Commun.*, (1986) 1327.
28 P. Chmielewski, M. Grzesczuk, L. Latos-Grazynski and J. Lisowski, *Inorg. Chem., 28* (1989) 3546.
29 M.I. Seullane and H.C. Allen, Jr., *J. Coord. Chem., 4* (1975) 255.
30 S. Gambarotta, F. Urso, C. Florian, A. Chiesi-Villa and C. Guastini, *Inorg. Chem., 22* (1983) 3966.
31 L. Horner and R.E. Schmitt, *Z. Naturforsch., Teil B, 37* (1982) 1163.